BMC Biology

RESEARCH

Open Access

Deformed wing virus coopts the host arginine kinase to enhance its fitness in honey bees (*Apis mellifera*)

Andrea Becchimanzi[1,2], Giovanna De Leva[1], Rosanna Mattossovich[3], Serena Camerini[4], Marialuisa Casella[4], Giovanni Jesu[1], Ilaria Di Lelio[1,2], Sabrina Di Giorgi[5], Joachim R. de Miranda[6], Anna Valenti[3*], Silvia Gigliotti[3*] and Francesco Pennacchio[1,2*]

Abstract

Background Deformed wing virus (DWV) is a major honey bee pathogen that is actively transmitted by the parasitic mite *Varroa destructor* and plays a primary role in *Apis mellifera* winter colony losses. Despite intense investigation on this pollinator, which has a unique environmental and economic importance, the mechanisms underlying the molecular interactions between DWV and honey bees are still poorly understood. Here, we report on a group of honey bee proteins, identified by mass spectrometry, that specifically co-immunoprecipitate with DWV virus particles.

Results Most of the proteins identified are involved in fundamental metabolic pathways. Among the co-immunoprecipitated proteins, one of the most interesting was arginine kinase (ArgK), a conserved protein playing multiple roles both in physiological and pathological processes and stress response in general. Here, we investigated in more detail the relationship between DWV and this protein. We found that *argK* RNA level positively correlates with DWV load in field-collected honey bee larvae and adults and significantly increases in adults upon DWV injection in controlled laboratory conditions, indicating that the *argK* gene was upregulated by DWV infection. Silencing *argK* gene expression in vitro, using RNAi, resulted in reduced DWV viral load, thus confirming that *argK* upregulation facilitates DWV infection, likely through interfering with the delicate balance between metabolism and immunity.

Conclusions In summary, these data indicate that DWV modulates the host ArgK through transcriptional regulation and cooptation to enhance its fitness in honey bees. Our findings open novel perspectives on possible new therapies for DWV control by targeting specific host proteins.

Keywords DWV, Iflaviridae, Protein–protein interaction, Mass spectrometry, ATP phosphotransferase, Honey bee cells, Metabolism-immunity crosstalk

*Correspondence:
Anna Valenti
anna.valenti@ibbr.cnr.it
Silvia Gigliotti
silvia.gigliotti@ibbr.cnr.it
Francesco Pennacchio
f.pennacchio@unina.it
Full list of author information is available at the end of the article

Background

Pathogenic viruses affecting honey bees are among the most intensively studied pathogens, given their great impact on beekeeping, as one of the main causes of honey bee (*Apis mellifera*) colony losses [1–3], and their potential negative impact on wild bees, through spill-over from beekeeping operations [4].

One of the most studied viral pathogens of honey bees is deformed wing virus (DWV; Iflaviridae), an endemic RNA positive single-stranded virus [5], which is vectored by the parasitic mite *Varroa destructor* [6–8]. At low viral loads, DWV is asymptomatic and nearly universally distributed in regions where Varroa is established [9–11]. However, when honey bee colonies are heavily infested by *V. destructor*, DWV rapidly spreads and the transition from common asymptomatic infections to devastating overt infections occurs [5, 12–15].

The increasing viral infection is a self-sustaining process, as the growing DWV titer generates an escalating immunosuppression, by targeting NF-kB signaling through an as-yet-unknown mechanism, which has devastating consequences for bee health [9, 16]. Understanding the molecular mechanisms underlying DWV infection, such as protein–protein interactions at the host–pathogen interface or co-infection dynamics with other pathogens [17–20], may offer the opportunity to develop new management strategies and therapeutic approaches based on, for example, RNA interference (RNAi) via administration of synthetic dsRNA to honey bee colonies [21–23].

The genomic RNA of DWV contains a single large open reading frame encoding a 328 kDa polyprotein. The DWV virion is constructed by three major structural proteins VP1, VP2, and VP3 [17], which map to the N-terminal section of the polyprotein (Additional file 1: Fig. S1). The C-terminal part of the polyprotein contains sequence motifs typical of well-characterized picornavirus nonstructural proteins: an RNA helicase, a chymotrypsin-like 3C protease, and an RNA-dependent RNA polymerase [24]. Studies on different iflaviruses indicate that structural proteins of iflavirus are associated with viral invasion and replication by interacting with host proteins [18, 25, 26]. These data suggest that the identification of host proteins interacting with the DWV structural proteins may help to clarify the infection process and pathogenesis of the virus.

Immunoprecipitation of protein complexes followed by electrophoretic separation of the co-precipitated proteins and mass spectrometry (IP-MS) analysis has proven an efficient approach to characterize the composition and function of protein complexes, including those involving infectious viruses [27], and is therefore a useful tool for studying host-virus interactions at the protein level.

Here, we applied this approach to DWV from naturally infected, symptomatic adult honey bees. This revealed a number of honey bee proteins associated with DWV particles. One of the most interesting of these proteins was arginine kinase (ArgK). ArgK is a highly abundant phosphotransferase found in invertebrate animals and bacteria that catalyzes the reversible phosphorylation of arginine residues with adenosine triphosphate (ATP) to produce phosphoarginine, which acts as a rapidly deployable energy reservoir for a range of biological and cellular functions, including response to environmental stressors. In this, it occupies a similar role to creatine kinase in vertebrates [28]. Several lines of evidence have demonstrated that phosphorylation regulates multiple properties of viral proteins, such as activity, stability, subcellular localization, and interaction with protein partners or nucleic acids, and thus plays a key role in the viral life cycle [29, 30].

Here, we report a functional characterization of the role of ArgK in modulating the honeybee-DWV interaction, as a strategy to identify possible targets for antiviral agents.

Results

Identification of honey-bee proteins interacting with DWV particles

We analyzed the presence of DWV structural proteins in total protein extracts from adult honey bees by western blot analysis, using a polyclonal antibody (DWV-Ab) directed against different DWV isolates. The antibody identified DWV capsid proteins in extract from symptomatic honey bees but not in extract from asymptomatic bees (Fig. 1A). The main band had a molecular mass of 45 KDa, corresponding to DWV VP3, as per consensus for picorna-like virus structural protein nomenclature (Additional File 1: Fig. S1) [31–33], while other bands at a lower molecular weight were compatible with VP2 and VP1, respectively. Original uncropped blot images are shown in Additional File 1: Fig. S2.

To investigate the role of DWV proteins in viral infection, we combined immunoprecipitation experiments with a proteomic approach aimed at identifying honey bee proteins forming molecular complexes with DWV. A mixture of protein extracts from symptomatic bees was used to perform immunoprecipitation, using either the DWV-Ab or a control antibody (C-Ab), both produced in rabbits. DWV-Ab specifically immunoprecipitated the DWV viral proteins, indicating that this antibody recognizes the viral proteins under native conditions (Fig. 1B).

Four independent co-immunoprecipitation experiments were carried out using both DWV-Ab (IP) and C-Ab (Ctrl). The eight co-precipitated protein samples thus obtained were individually separated by

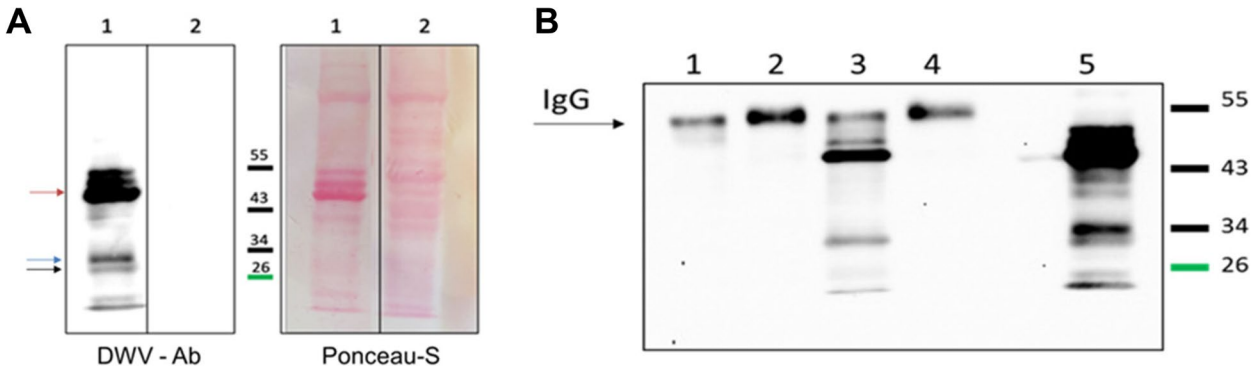

Fig. 1 Immunoprecipitation of viral particles. **A** Western blot analysis of total protein extracts (15 ug) prepared from symptomatic (lane 1) or asymptomatic (lane 2) bees. The membrane was incubated with DWV-Ab and stained with Ponceau-S. The antibody specifically recognizes viral proteins in the total protein extract of symptomatic honey bees. The arrows indicate the main viral proteins found in the extracts of symptomatic honey bees at MW of VP3 (red), VP2 (blue), and VP1 (black). **B** Western blot analysis of immunoprecipitation. IP was performed from pooled protein extracts of symptomatic honey bees using the DWV-Ab (lane 3) or a control antibody C-Ab (lane 4). DWV-Ab and C-Ab were loaded in lanes 1 and 2, respectively, as a control of migration. The capsid proteins were visualized using the DWV-Ab. The arrow indicates the migration of IgGs. Lane 5 shows the input protein extract

SDS-PAGE (Fig. 2A). Each lane was divided into six fractions (48 fractions in total) and each fraction was analyzed by LC–MS/MS. After filtering for contaminants, a total of 223 protein sequences were identified in the IP samples: 193 matching with *Apis mellifera* proteins and the remaining all corresponding to the DWV polyprotein or parts of it (Additional File 2: S1 Dataset). Peptide alignments mainly revealed the complete VP2-VP3-VP1 structural DWV particle block and fragments of the DWV helicase. Just one of the peptides aligns in the DWV RNA-dependent RNA polymerase (RdRp).

The quantitative data acquired for all proteins were statistically analyzed, using a principal component (PC) analysis (Fig. 2B). The PC analysis showed a clear separation between IP and Ctrl samples with a good reproducibility among biological replicates. A *t*-test was applied and identified 142 honey bee proteins that were significantly enriched in the IP samples (Additional File 3: S2 Dataset and Fig. 2C).

To obtain an overview of the putative functions of the identified honey bee proteins, GO enrichment analysis was performed on the proteins enriched in the IP samples. This revealed that 111 proteins are associated to enriched GO terms. DAVID clustering (Additional File 4: S3 Dataset) revealed that enriched GO terms are mainly related to translation (GO:0003743 ~ translation initiation factor activity; GO:0006412 ~ translation; GO:0005840 ~ ribosome), catabolism of aberrant proteins (GO:0036402 ~ proteasome-activating ATPase activity; GO:0030163 ~ protein catabolic process), cell structure (GO:0005200 ~ structural constituent of cytoskeleton; GO:0005874 ~ microtubule), and protein transport (GO:0006886 ~ intracellular protein transport; GO:0016192 ~ vesicle-mediated transport) (Fig. 2C).

Characterization of Arginine kinase role in DWV infection

Among all the proteins that were enriched in the IP sample, the honey bee Arginine kinase (ArgK) was selected for functional analyses. Several reasons prompted this investigation. ArgK is an important member of the phosphagen kinase family, extensively studied in various vertebrates and invertebrates. There is evidence that many viruses interact with, and hijack, cellular kinases for their replication, transcription, and assembly [30, 34]. However, no information is available about ArgK function in the honey bee-DWV interaction, in spite of the fact that, by modulating the intracellular levels of ATP, it can have an impact on ATP-sensitive inwardly rectifying potassium (K_{ATP}) channels, which are involved in the regulation of antiviral immune response in honey bees [35, 36] and in *Drosophila* [37]. Moreover, this enzyme is upregulated under stress conditions in insects, including pathogen infection [38–41]. Therefore, it is plausible that ArgK could be involved in the DWV virulence strategy. In particular, the role(s) it plays in the modulation of the host stress response could shed new light on the synergistic interaction of multiple stress agents, which negatively impact on host immunocompetence and trigger the progression of latent DWV infections [9, 16, 19, 42–47].

To investigate this hypothesis, we first characterized the expression profile of the *argK* gene in different host tissues and developmental stages. RT-qPCR analysis indicated that the *argK* gene is highly transcribed in the brain of newly emerged adult bees (Fig. 3A), more than tenfold

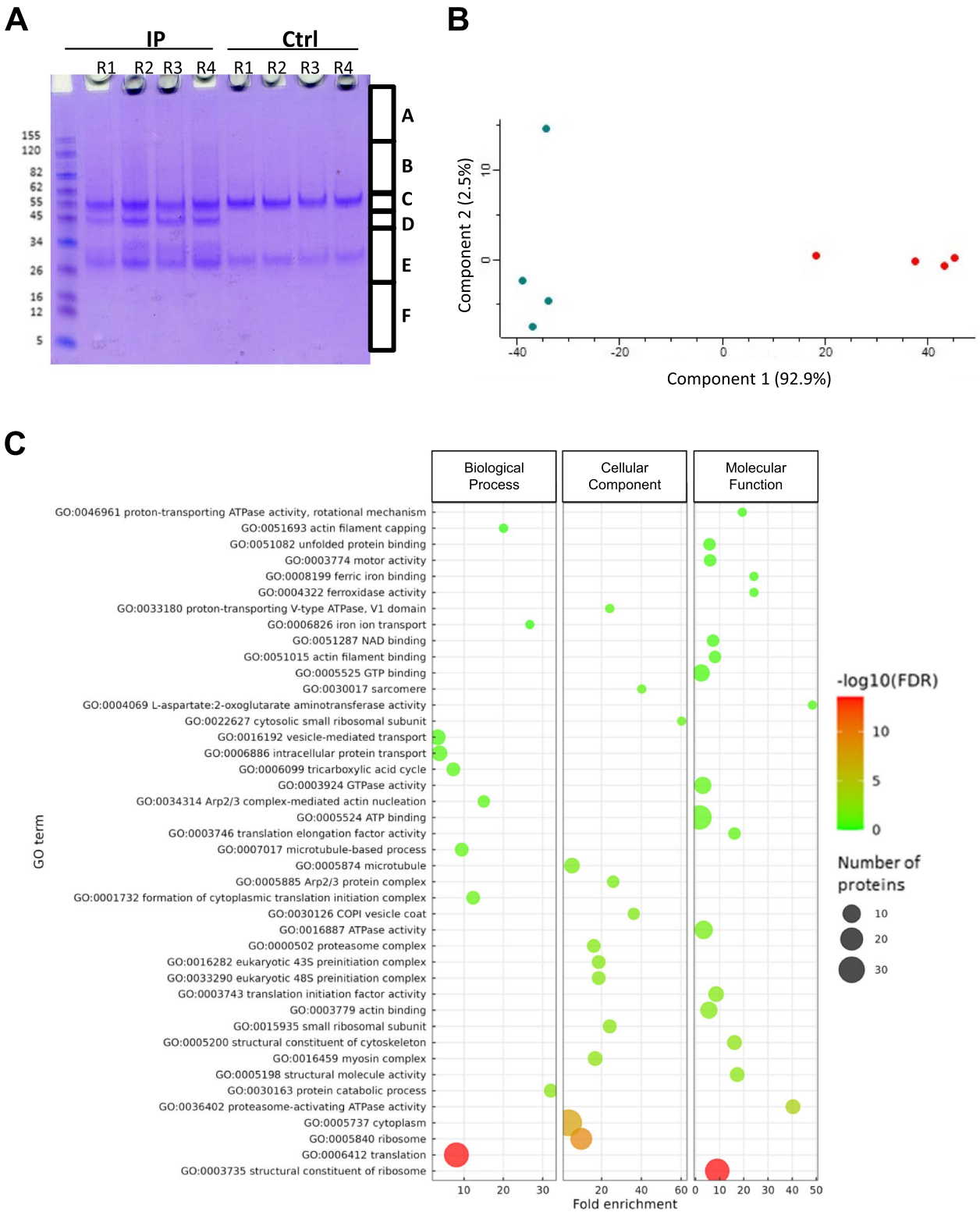

Fig. 2 Identification of DWV-interacting proteins in honey bees. **A** Coomassie-stained gel in which immunoprecipitated proteins were separated. R1, R2, R3, and R4 indicate the four biological replicates for control (Ctrl) and target (IP) samples. A, B, C, D, E, and F indicate the slices cut for each lane, which were defined to separate intense bands, containing the most abundant proteins, from faint ones, containing low represented proteins. **B** PCA analysis of quantitative data obtained from LC–MS/MS. Green and red dots indicate Ctrl and IP sample replicates, respectively. **C** GO terms enriched in DWV-Ab samples. *X*-axis indicates fold enrichment calculated by DAVID enrichment tool, using the whole set of proteins of *A. mellifera* as background dataset. Bubble diameter and color indicate number of proteins and negative false discovery rate (FDR), respectively

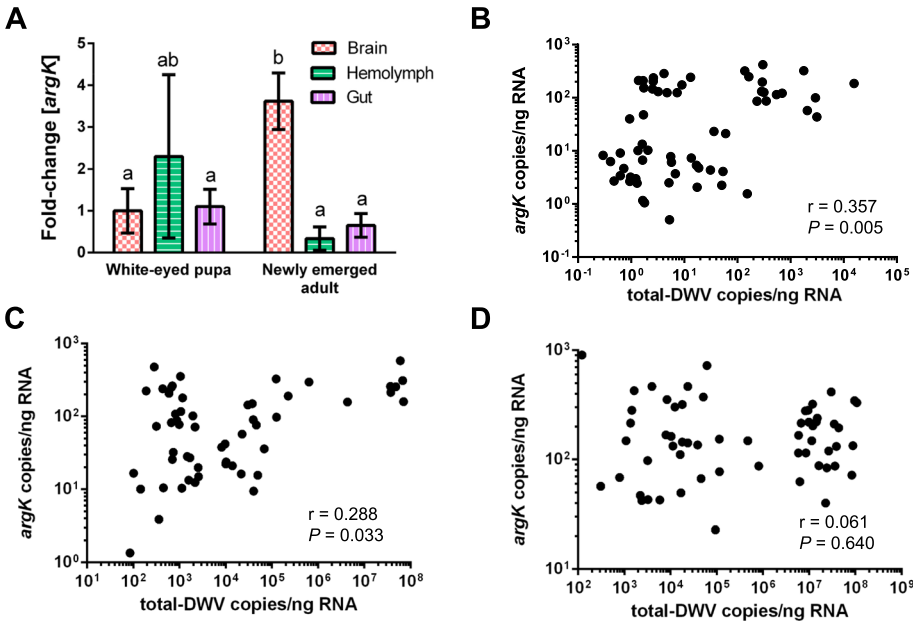

Fig. 3 *argK* expression in field-collected honey bees. **A** *argK* transcript levels in pupal and adult tissues. *argK* gene expression was significantly higher in the adult brain, compared with the other tissues analyzed (two-way ANOVA and Holm-Sidak post hoc analysis, see Additional file 1: Table S3). Two-way ANOVA revealed that there was a statistically significant interaction between the sampled tissue and insect development ($F(2, 17) = 12.76$, $P = 0.0004$). Simple main effects analysis showed that sampled tissue had a significant effect ($F(2, 17) = 4.78$, $P = 0.022$), while insect development did not have a significant effect on *argK* transcription ($P = 0.862$). Error bars indicate standard deviation; statistically significant differences are denoted with different letters ($P < 0.05$). **B**–**D** Expression of *argK* is positively correlated with total-DWV load (Spearman's rank correlation, $r > 0$, $P < 0.05$, $n = 55$) in larvae (**B**) and nurse bees (**C**), but not in foragers (**D**). DWV and *argK* copies were normalized on the nanograms of total RNA. Values on *X*- and *Y*-axis are reported in Log10 scale. Exact Spearman's rank correlation coefficient (*r*) and *P*-values (*P*) are reported in the figures

compared to adult hemolymph and gut samples. In the pupal stage, a completely different pattern was observed, with a reduced expression in brain and no statistical differences between sampled tissues (S3 Table). Spearman's rank correlation test revealed that *argK* expression and DWV load were positively correlated in field-collected larvae and nurse bees (Fig. 3B and C), while no correlation was observed for foragers (Fig. 3D).

To assess the effect of DWV infection on *argK* expression, we performed RT-qPCR experiments on adult bees injected with a known dose of DWV particles (10^4 copies/bee). DWV load of DWV-injected bees ranged between 10^6 and 10^7, while PBS-injected bees showed a range between 10^2 and 10^5.

In artificially infected bees, high DWV loads were associated with an enhanced expression of *argK*, which was approximately twofold higher in DWV-injected bees than in non-injected (NI) and PBS-injected (PBS) bees. Spearman's rank correlation test revealed that *argK* expression and DWV load were positively correlated (Fig. 4).

To assess *argK* involvement in DWV infection, we performed in vitro gene knockdown studies in artificially DWV-infected primary cultures of honey bee pupal cells. The choice of an in vitro system was prompted by

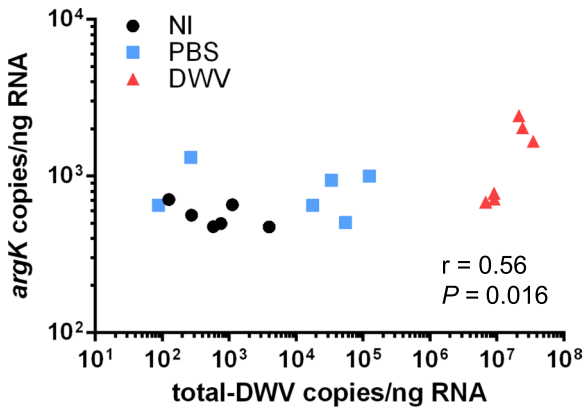

Fig. 4 Effect of controlled DWV infection on *argK* expression in artificially infected honey bees. Transcription of *argK* is positively correlated with total DWV load (Spearman's rank correlation, $r = 0.56$, $P < 0.05$, $n = 18$) in honey bees subjected to different treatments at the emergence. NI: non-injected; PBS: injected with PBS; DWV: injected with 10^4 DWV copies. Bees were sampled after 3 days from the treatment, and absolute quantification of *argK* and DWV copies was performed by RT-qPCR. Data were normalized on the nanograms of total RNA. Values on *X*- and *Y*-axis are reported in Log10 scale. Exact Spearman's rank correlation coefficient (*r*) and *P*-values (*P*) are reported in the figure

the broad involvement of ArgK in stress responses [41], which are much more difficult to control in naturally infected bees, with the risk that stress-related ArgK dynamics may mask any specific effect ArgK may have on DWV replication. Five days after dsRNA administration, *argK* was significantly downregulated (sevenfold) in *argk* dsRNA-treated cells (Fig. 5A), a condition that was associated with a threefold reduction of DWV load, relative to DWV-infected cells treated with a non-specific control dsRNA, against green fluorescent protein (GFP), a synthetic gene not naturally present in bee tissues (Fig. 5B). This result was associated with unaltered expression levels of the internal reference gene (*β-actin*), which indicates that the *argK* silencing does not affect cell viability (Additional File 1: Fig. S3).

Discussion

Due to its causal association with honey bee colony losses, DWV has been the subject of wide-ranging and extensive studies [7]. Nonetheless, knowledge on the molecular strategies adopted by this major honey-bee pathogen to bind, enter, and replicate in the host's cells is still limited [17].

As obligate intracellular parasites, viruses rely on the exploitation of host factors to establish a successful infection. Indeed, viral infection and replication are strictly dependent on virus-host protein–protein interactions. Hence, the identification of molecular interactors is essential to understand the mechanism of viral pathogenesis and for developing targeted antiviral strategies. Accumulating evidence, mostly deriving from investigation on mammalian RNA viruses, indicates that viral structural proteins forming the capsid that encloses the viral genome play a key role at all stages of the viral life cycle and can regulate distinct cellular processes by interacting with host factors [48].

DWV viral particles consist of a pseudo-T3 icosahedral capsid comprising 60 asymmetric units made of three proteins, VP1, VP2 and VP3, assembled in 12 pentameric structures around a positive-strand RNA genome [17, 49]. Our research on DWV-honey bee interaction shows that these DWV structural proteins are specifically recognized in the extracts of DWV-symptomatic bees by IgGs obtained from an antiserum generated against DWV viral particles. This allowed us to perform immunoprecipitation experiments, obtaining the molecular complexes formed by viral proteins and host factors.

LC–MS/MS analyses of the protein complexes confirmed the presence of the VP1, VP2 and VP3 structural proteins and identified 142 honey bee proteins. Two of them, 40S ribosomal protein S7 and elongation factor 1-alpha, had been previously found as VP2 interactors in *Apis cerana* [26, 50].

From a functional point of view, the honey bee proteins found in the co-immunoprecipitated complexes were mostly related to translation, catabolic functions, cytoskeleton structure, and protein transport. Close inspection of this protein list revealed the presence of several enzymes that are well-known components of the main pathways of central carbon metabolism: glycolysis (glyceraldehyde-3-phosphate dehydrogenase, phosphoglycerate mutase, ATP-dependent 6-phosphofructokinase), tricarboxylic acid cycle (citrate synthase, isocitrate dehydrogenase, oxoglutarate dehydrogenase), and pentose phosphate pathway (6-phosphogluconate dehydrogenase). This finding correlates with previous reports on the active recruitment of glycolytic and fermentation enzymes by plant viruses [51–53]. It was demonstrated

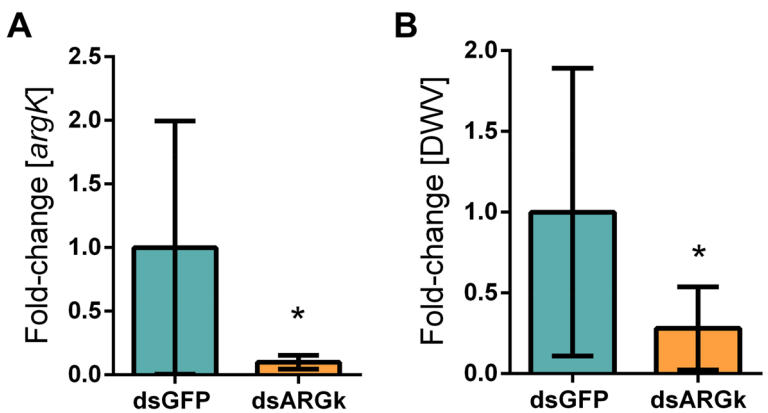

Fig. 5 Effect of *argK* knockdown on DWV load in honey bee cells. **A** *argK* transcription level was significantly lower in honey bee cells treated with dsRNA targeting *argK* (dsARGk), compared with cells treated with a control dsRNA (dsGFP) (Student's *t*-test: $t_{(14)} = 2.744$, $n = 7$). **B** In *argK*-silenced honey bee cells (dsARGk), DWV relative abundance was significantly lower, compared with control cells (dsGFP) (Student's *t*-test: $t_{(14)} = 2.323$, $n = 7$). * $P < 0.05$. Error bars indicate standard deviation

that tomato bushy stunt virus (TBSV) co-opted these enzymes within specialized viral replication organelles, to support robust viral RNA synthesis [54]. Analogous replication compartments were found in viruses infecting animals and were considered a hallmark of positive strand RNA viruses [55]. In addition, it was shown that hepatitis viruses actively manipulate the host metabolism through molecular interactions with specific enzymes such as glucokinase, the first rate-limiting enzyme of glycolysis [56, 57]. Therefore, we hypothesized that association of DWV capsid proteins with cellular enzymes responsible for the conversion of sugars into energy and metabolic precursors may target the host metabolism at critical nodes, redirecting the energy flux to support the progression of viral infection.

To start investigating if and how the host metabolic enzymes enriched in our IP samples are relevant for DWV infection, we selected one of these (ArgK) for functional analyses. This choice was based on the critical role ArgK plays in energy homeostasis in invertebrates, by catalyzing the transfer of a phosphate group between ATP and arginine [58]. The reversible nature of this reaction allows the synthesis of a metabolically inert pool of phosphorylated arginine during basal metabolic conditions, which is used to quickly replenish ATP stores during periods of high metabolic activity. Therefore, ArgK function is particularly relevant in tissues with high and fluctuating energy demands, such as muscles and nervous system [59–61]. This is consistent with our finding that the gene encoding for ArgK is highly transcribed in the brain of adult bees, where DWV actively replicates [62]. Moreover, regulation of intracellular ATP levels by ArgK activity can have an impact on antiviral immunity, as suggested by the role played by ATP-sensitive potassium channels in the modulation of insect antiviral barriers [35–37].

As a first step in the functional characterization of the DWV-ArgK interaction in honey bees, we performed a population survey aimed at evaluating the relationship between DWV infection and *argK* transcript accumulation. The obtained results indicated that higher DWV load is associated with higher levels of *argK* transcript in honey bee larvae and nurse bees. The same pattern is not observed in foragers, likely due to other factors affecting *argK* expression, such as aging, strenuous energetic activity (flight and foraging), or exposure to environmental stressors [41]. The positive correlation between *argK* and DWV levels was confirmed by artificial in vivo infection experiments, indicating that DWV inoculation triggers *argK* gene transcription in honey bees.

Since ArgK is a phosphagen kinase controlling ATP production and utilization, increased expression of the *argK* gene, along with association of the ArgK enzyme with DWV capsid proteins, may have a strong impact on progression of DWV infection. As a major source of energy in the cell, ATP is in fact required in different processes occurring during the life cycle of viral pathogens [63]. For instance, it has been demonstrated that transcriptional initiation and replication of RNA viruses are ATP-dependent processes [64–66]. ATP is also required for the unwinding of viral genomes by helicase enzymes [67]. Finally, it has been shown that ATP is involved in the assembly and/or disassembly of viral particles [68, 69].

Therefore, a functional interaction with ArgK may be a strategy developed by DWV to regulate local ATP levels, thus acquiring the energy resources necessary for progression of viral infection. By using this strategy, DWV could take advantage from upregulation of the *argK* gene, which is a common response elicited by different stress conditions in invertebrate species [41, 70, 71]. Indeed, increase of *argK* transcription was found to be associated with a switch in the direction of the enzymatic reaction catalyzed by the ArgK enzyme in *Tribolium castaneum*, to produce ATP from the phosphoarginine pool [72].

Modulation of the ATP/ADP ratio by ArgK activity may also affect the function of ATP-dependent cellular factors involved in virus-host dynamics. Among them, likely candidates are ATP-sensitive potassium (K_{ATP}) channels, which play a crucial role in antiviral immunity in honeybees [35, 36], and, more in general, in insects [37, 73]. In fact, it can be hypothesized that increased ATP production by ArgK results in reduced activity of K_{ATP} channels (which are indeed inhibited by ATP), thus leading to viral outbreak.

Our data support this hypothesis, showing that downregulation of *argK* expression by RNAi reduces viral load under experimental in vitro infection, thus demonstrating that ArgK positively modulates the progression of DWV infection. Future experiments will allow testing the existence of a functional relationship between ArgK and K_{ATP} channels in honey bees, a possibility that is also suggested by previous investigation on creatine kinase, the main vertebrate phosphagen kinase, which physically associates with K_{ATP} channels and regulates their behavior [74, 75].

Moreover, it is worth noting that this regulatory strategy might have a broader impact on immune response. The central role of K_{ATP} channels in regulating the metabolic homeostasis underlying well-being under stress appears to be conserved, as suggested by evidence available for mammals and insects [37, 73, 76, 77], and seems to have an influence on multiple signaling pathways controlling inflammation and human immunity [78]. This is a very interesting research area, which will likely contribute to unravel the complex synergism among different stress

agents, contributing to immune suppression and health decline of honey bee colonies [9, 16, 19, 42–47]. The present study is a first step in this direction, establishing a direct role of the virus in the manipulation of the delicate balance between metabolism and immunity, which was already proposed more than 10 years ago, based on compelling indirect evidence [16]. Now, we have an interesting molecular scenario to investigate, which will allow to better understand and hopefully manage pharmacologically the widespread phenomenon of honey bee colony losses, and, more in general, the animal response to stress using insects as an amenable model system.

In addition to the functional scenario outlined above, the possibility that ArgK may act as a noncanonical receptor involved in viral binding and entry cannot be ruled out and is certainly worth of future research efforts. However, our current data do not allow to determine whether ArgK directly interacts with DWV capsid proteins or whether the interaction is mediated by other proteins.

The results of the present study shed light on the molecular mechanism accounting for the recently observed reduction of DWV load in cultured honey bee head tissues treated with quercetin [79]. Quercetin is a known antiviral drug with strong inhibitory activity towards ArgK of *Locusta migratoria manilensis* by binding to Trp residues in the active site [80]. Our findings suggest that honey bee ArgK is one of those host's proteins to which quercetin binds, resulting in the inhibition of DWV replication in vitro [79].

In another work on ArgK implication in viral infection, this enzyme was reported as a target for a DNA virus, the white spot syndrome virus (WSSV), which infects several shrimp species [34, 81]. By interacting with WSSV envelope proteins, shrimp ArgK resulted in increased viral titer in either *Litopenaeus vannamei* or *Marsupenaeus japonicus* [34, 81]. Notably, ArgK enzymatic activity was necessary for successful progression of WSSV infection in the latter system, as WSSV proliferation decreased when a mutant form of ArgK carrying a deletion in the active site was injected in shrimps, or a selective inhibitor was used to suppress the kinase activity of the enzyme [81].

Exploitation of ArgK by both DWV and WSSV is a novel example of evolutive convergence in the strategies used by phylogenetically unrelated viruses to hijack host cellular functions. In this context, it is interesting to note that also another phosphagen kinase, creatine kinase B (CKB), was previously implicated in virus pathogenicity. CKB plays in vertebrates the same role as ArgK in invertebrates that is coupling energy production with cellular function [58]. To perform this task, CKB catalyzes the reversible transfer of the phosphate group of phosphocreatine to ADP, generating creatine and ATP. During human hepatitis C virus infection (HCV), CKB binds to the NS3-4A complex formed by two viral nonstructural proteins and upregulates both the viral RNA and DNA unwinding and the replicase activity of this complex, ensuring efficient replication and propagation of the virus [82]. In addition, contribution of a CKB enzyme to viral replication was reported also in grouper fish infected by the nervous necrosis virus (NNV) [83].

Conclusions

In conclusion, the finding of ArgK as a honey bee protein recruited by DWV to promote its own replication adds a new piece of information to our understanding of this specific host-virus interaction system. It also represents a case report about the ability of pathogenic viruses to hijack the host metabolic machinery, which is an emerging issue in viral biology. Finally, our results provide a promising target for the future development of therapeutic approaches aimed at reducing the impact of DWV on honey bee populations, thus contributing to preserve pollinators health.

Methods

Biological material

A. mellifera colonies were maintained at the experimental apiary of the Department of Agricultural Sciences (University of Napoli Federico II), based in Portici (Napoli, Italy). Adult bees and brood frames were collected between June and August 2020 and stored at 32 ± 1 °C, 60 ± 2% relative humidity, under dark conditions.

Protein isolation

Symptomatic and asymptomatic adult honey bees were collected from highly infested and *Varroa*-free apiaries, respectively, and stored at − 80 °C until protein extraction. Individual honey bees were processed in different microcentrifuge tubes containing 500 µl phosphate buffered saline (PBS; 137 mM NaCl, 8.1 mM Na_2HPO_4, 2.68 mM KCl, 1.47 mM KH_2PO_4, pH 7.4) + protease inhibitor cocktail (cOmplete™, Mini, EDTA-free Protease Inhibitor Cocktail, Roche, Basel, Switzerland). The tissues were ground by hand using plastic pestles, centrifuged for 5 min at 13,000 g at 4 °C, and the aqueous part was then transferred to fresh tubes, leaving tissue debris pellet behind. The protein extracts were stored in 20% glycerol at − 80 °C. The pelleted debris was processed to isolate RNA using TRIzol reagent (Thermo Fisher Scientific, Waltham, MA, USA), in order to confirm the DWV status of the DWV-infected and DWV-free samples by RT-qPCR, as described below.

Serology and antibody production

The polyclonal DWV antiserum (DWV-Antiserum; #213–3) was raised in 1985 against a Japanese isolate of DWV, by immunizing a white rabbit through intramuscular injection with 1 mg purified DWV particles, followed by two booster injections of 0.1 mg virus emulsified in an equal volume of Freund's adjuvant [31]. At 2–4-week intervals after the final booster immunization, blood was drawn from the marginal vein of the rabbit's ear, from which the serum fraction was separated using standard procedures [84] and titrated against the original DWV antigen. In 1998, anti-DWV IgG (DWV-Ab; #164/H) was purified from the antiserum on a protein-A agarose column using standard procedures [84].

Western blot

Total protein extracts from symptomatic and asymptomatic honey bees, obtained by pooling separately the DWV-infected and DWV-free samples, were analyzed by western blot, to check for the presence of DWV structural proteins. Samples were run in 8% polyacrylamide gels in 1×Tris–Glycine-SDS Running buffer (25 mM Tris, 192 mM glycine and 0.1% SDS, pH 8.3). After electrophoresis, proteins were transferred onto PVDF filters (Bio-Rad, Hercules, CA, USA) using the Trans-Blot1 TurboTM Blotting System (Bio-Rad). Subsequently, the PVDF membrane was stained with Ponceau-S, rinsed with water and scanned to save the staining image. The Ponceau-S stain was then removed from stained proteins by washing the PVDF membrane in PBS containing 0.1% Tween® 20 (PBST), several times for 5 min under shaking. Subsequently, the PVDF membrane was incubated with the PVDF blocking reagent (PBST supplemented with 5% milk; Bio-Rad) for 60 min at room temperature (RT) and washed thrice in PBST for 5 min with shaking. After blocking, the PVDF membrane was incubated for 1 h at RT in PBST containing DWV-Ab at 1:2,000 dilution, followed by a second incubation of 1 h at RT with a secondary commercial anti-Rabbit antibody conjugated to horseradish peroxidase (Pierce/Thermo Scientific) at 1:50,000 dilution in PBST. After rinsing in PBST, the PVDF membrane was incubated with ECL-plus solution (Biosciences, Town, Country) to reveal the chemiluminescent bands produced by the HRP, which were captured photographically using a VersaDoc apparatus (Bio-Rad, Town, Country).

Immunoprecipitation

Immunoprecipitation (IP) experiments were performed using the DWV-Ab and protein extracts from symptomatic or asymptomatic honey bees. Control IP experiments were performed using control IgG purified from a rabbit antiserum produced against a bacterial protein (C-Ab). All IP steps were carried out on ice or at 4 °C using freshly thawed protein extracts and Buffers and in the presence of protease inhibitors, accordingly to manufacturer's instructions (Protein A Agarose; Code: 11,134,515,001; Roche). To reduce the binding of non-specific proteins to the beads, the protein extracts (0.5 mg) were first incubated with protein A agarose (60 µl) for 2 h at 4 °C with gentle agitation; afterwards, each sample was centrifuged accordingly to manufacturer's instructions. Half of the soluble fraction was incubated with DWV-Ab and the other half with C-Ab, both for 1 h at 4 °C. After incubation, 30 µl of protein A agarose was added to each sample and incubated O/N at 4 °C in washing buffer 1 (50 mM Tris–HCl, pH 7.5; 150 mM sodium chloride; 1% Nonidet P40; 0.5% sodium deoxycholate; 1 tablet complete protease inhibitor cocktail/50 ml). After incubation, the sample was centrifuged at 12, 000 g for 30 s, and the resin was washed two times for 20 min at 4 °C with 0.5 ml of washing buffer 1, two times with 0.5 ml of washing buffer 2 (50 mM Tris–HCl, pH 7.5; 500 mM sodium chloride; 0.1% Nonidet P40; 0.05% sodium deoxycholate), and once with 0.5 ml of buffer 3 (50 mM Tris–HCl, pH 7.5; 0.1% Nonidet P40; 0.05% sodium deoxycholate). Finally, co-immunoprecipitated proteins were eluted by using 0.1 M glycine•HCl buffer, pH 2.5–3.0 and analyzed by SDS-PAGE and western blot as described above. For mass spectrometry analysis, four independent coIP experiments (both for sample and control) were performed and an aliquot was analyzed by western blot to check for the presence of virion proteins. The co-immunoprecipitated proteins were separated by SDS-PAGE and subjected to mass spectrometry analysis as described below.

LC–MS/MS

The DWV-Ab and control immunoprecipitated samples, each in quadruplicate, were separated in a precast polyacrylamide gradient (4–12%) gel (Invitrogen, Carlsbad, CA, USA), run in MES buffer (Invitrogen) for 25 min at 200 V, and the proteins were stained with the Imperial Coomassie stain (Invitrogen). Each of the 8 lanes was divided into 6 bands, i.e., 48 bands in total, which were destained with 50 mM ammonium bicarbonate and acetonitrile (ACN) 1:1 (v/v), treated for cysteine reduction (10 mM dithiothreitol at 56 °C for 45 min) and alkylation (55 mM iodoacetamide at RT for 30 min in the dark) and for enzymatic digestion with 12.5 ng/µl trypsin (Promega Corporation, WI, United States) at 37 °C overnight. The resulting peptide mixture was analyzed by LC–MS/MS using an Ultimate 3000 HPLC coupled with an Orbitrap Fusion Tribrid (Thermo Fisher Scientific). Peptides were desalted on a trap column (Acclaim PepMap 100 C18, Thermo Fisher Scientific) and separated on a 19-cm-long

silica capillary (MS WIL, Aarle-Rixtel the Netherlands), packed in-house with a C18, 1.9 microm, 100 Angstrom resin (Michrom BioResources, CA, United States). The analytical column was encased by a column oven (Sonation; 40 °C during data acquisition) and attached to a nanospray flex ion source (Thermo Fisher Scientific). Peptides were separated on the analytical column by running a 95 min gradient of buffer A (5% ACN, and 0.1% formic acid) and buffer B (95% acetonitrile and 0.1% formic acid), at a flow rate of 250 nl/min. The mass spectrometer operated in positive ion mode, and full MS was acquired in the Orbitrap in the m/z 350–1550 scan range at 120 K resolution. Data-dependent acquisition was performed in top-speed mode (3 s long maximum total cycle): the most intense precursors were selected through a monoisotopic precursor selection (MIPS) filter and with charge > 1, quadrupole isolated (1.6 m/z width) and fragmented by 30% higher-energy collision dissociation. Product ion spectra were acquired in the ion trap with rapid scan rate.

Peptide spectra were analyzed with Proteome Discoverer 2.4 (Thermo Fisher Scientific) by the search engine Sequest HT using a mixed database containing *Apis mellifera* (20,818 reviewed and unreviewed sequences; release 26/01/2022), *Homo sapiens* (42,253 sequences, v2017-10–25) *Oryctolagus cuniculus* (892 sequences, release 07/03/2022), and Deformed Wing Virus (1067 sequences, release 26/01/2022), all downloaded from Uniprot (https://www.uniprot.org/).

Precursor and fragment mass tolerance were set to 15 ppm and 0.6 Da, respectively. Cysteine carbamydomethylation was set as static modification, while methionine oxidation and N-acetylation on protein terminus were set as variable modifications. Specific trypsin cleavages with maximum two miscleavages were admitted. Spectral matches were filtered at 1% false discovery rate (FDR), based on *q* values, and target-decoy approach, using the Percolator node. Only master proteins were taken into account. Quantification was based on precursor intensity of unique and razor peptides.

Bioinformatic analysis

MS spectra were analyzed by the Proteome Discoverer software identifying 405 proteins of which 372 were also quantified. The Perseus software (1.6.15) was used to perform statistical analyses and evaluate differential protein abundance. After contaminant removal (rabbit and human proteins), the abundance values were log2 transformed and filtered for containing at least four valid values in at least one group. Missing values were imputed with the constant value 13. A Student's *t*-test was performed applying 250 randomizations, setting S0 = 2 and 0.01 FDR. A PCA (principal component analysis) analysis was performed using the Perseus software.

DAVID enrichment tool [85] was interactively run through the DAVID web interface (https://david.ncifcrf.gov/), using the whole dataset of *A. mellifera* proteins as background. Results for the annotation categories GOTERM_BP_DIRECT, GOTERM_MF_DIRECT, and GOTERM_CC_DIRECT were collected for analysis and visualized using *ggplot2* package through R software (version 4.0.3).

argK mRNA expression and DWV load in field-collected bees

To localize *argK* mRNA expression, honey bee pupae and newly emerged bees (NEB) were dissected using microforceps, under a stereomicroscope (SteREO Discovery V8, Zeiss, Jena, Germany). Brain, hemolymph, and gut samples were collected in microcentrifuge tubes containing TRIzol reagent (Thermo Fisher Scientific). To study the relationship between DWV infection and *argK* expression in field conditions, we sampled mature larvae (4–5 days from hatching), nurse bees, and foragers from two hives. Nurse bees were identified by observing their activity of nursing immatures on the frame. The two hives were in similar conditions of strength and provisions. Sampled bees and tissues were stored at – 80 °C until RNA extraction.

Controlled DWV infection in vivo

To assess the effect of DWV infection on *argK* expression, we artificially infected NEB with semi-pure DWV and maintained them under controlled conditions. NEB were injected with a DWV lysate prepared as described elsewhere [86]. Briefly, adult bees with symptomatic DWV infection were homogenized in 500 µl PBS in 1.5 ml microcentrifuge tubes. Tubes were centrifuged at 14,000 g for 10 min at 4 °C, and supernatant was clarified by adding an equal volume of chloroform. Samples were vortexed for 30 s, centrifuged at 10,000 g for 10 min at 4 °C, and supernatants were filtered through 0.22-µm sterile syringe filters (VWR, Radnor, Pennsylvania, USA). Lysates were stored in 40% glycerol at – 80 °C until use. RNA isolated from a subsample of the viral lysates was evaluated for DWV load by RT-qPCR, as described below, and for the presence of other common bee viruses by PCR, as described elsewhere [87]. NEB were cold-anesthetized at – 20 °C for 3 min and then either injected (or not) with 2.5 µl of 1X PBS containing 10^4 DWV copies, under a stereomicroscope (SteREO Discovery V8, Zeiss, Jena, Germany). The viral lysates were injected between the 4th and 5th abdominal segments using a beveled 33G NanoFil Needle (NF33BV-2) mounted on a 10-µl NanoFil syringe (World Precision Instruments,

Berlin, Germany). After injection, each bee was manually fed 5 µl of honey bee gut homogenate, using a micropipette, to establish the same characteristic gut community in experimental individuals, as described elsewhere [88–90]. This step is important because emerging bees lack their gut microbiome. In a hive, this is quickly supplied by interaction with older worker bees [88], but in laboratory settings, this needs to be supplied experimentally, to avoid gut dysbiosis with a possible negative impact on their health and unclear (and avoidable) disturbing factor during the bioassay experiment. The freshly prepared gut homogenates were obtained by pulling the intestines from four nurse bees, homogenizing these in 500 µl 1X PBS, and diluting the homogenate 1:1 with 50% filtered sucrose/water solution. DWV-injected and non-injected controls were confined in separated disposable plastic cages (28×11x11 cm) and provided with pollen paste (90% w/w fresh corbicular pollen with water) and 50% filtered sucrose/water solution (w/v) ad libitum, inside an incubator at the abovementioned conditions. After 3 days, the experimental bees were sampled and stored at −80 °C until dissection.

dsRNA synthesis

Gene-specific primers flanked by T7 promoter sequences (F: TAATACGACTCACTATAGGGAGAATTTGCTGACCTCTTCGACCC; R: TAATACGACTCACTATAGGGAGAAAAACCTGTCCAAGGTCACCG) were designed in order to amplify a 496-bp fragment of *argK* (AF023619.1), to be used for in vitro synthesis of dsRNA molecules. This fragment of the *argK* gene is distinct from the fragment targeted by the RT-qPCR primers used to evaluate the *argK* mRNA expression levels, such that the dsRNA used in silencing experiments should not be detected by the diagnostic *argK* mRNA expression assay.

The DNA sequences, serving as templates for dsRNA production, were generated through PCR amplification. The RNA extracted from adult honey bees was retrotranscribed with High-Capacity cDNA RT Kit according to manufacturer's instructions (Thermo Fisher Scientific). The resulting cDNA was used as template (2 µl) for PCR reactions containing the following components: 25 µl Phusion Flash High-Fidelity PCR Master Mix (Thermo Fisher Scientific), the two primers at 500 nM final concentration, and nuclease-free water to a total volume of 50 µl. The cycle conditions were as follows: 10 s at 98 °C; 1 s at 98 °C, 5 s at 66 °C and 15 s at 72 °C for 5 cycles; 1 s at 98 °C and 15 s at 72 °C for 30 cycles. Four separate reactions were pooled to produce at least 1 µg of the amplicon, the minimum required for subsequent dsRNA synthesis. A sample of the amplified products was run on a 1% agarose gel to verify that the PCR reaction produced a single band of the expected size. The amplified products were then purified with PureLink PCR Purification Kit (Thermo Fisher Scientific), eluted in nuclease-free water, and quantified measuring the absorbance with Varioskan Flash (Thermo Fisher Scientific). Following the manufacturer's instructions (MEGAscript RNAi kit, Thermo Fisher Scientific), the transcription reactions were assembled using 1.2 µg of purified PCR product. After DNA and ssRNA digestion, the dsRNA was purified and eluted in 50 µl of a 0.9% NaCl solution. The dsRNA concentration was determined spectrophotometrically, and the quality checked on a 1% agarose gel. A GFP dsRNA, exploited in control experiments, was similarly produced starting from the cloning vector pcDNA 3.1/CT-GFP TOPO (Thermo Fisher Scientific), which was used as template for a PCR reaction, performed as described elsewhere [91].

Honey bee cell culture

To investigate the role of *argK* in the DWV infection process, we used an in vitro system based on culturing primary honey bee pupal cells, as described elsewhere [92, 93]. To collect pupal cells, white eye stage pupae were carefully removed from comb cells using soft tip forceps and surface-sterilized in a sterile polystyrene petri dish (100 mm×15 mm, Fisher), in which pupae were swirled in 0.6% hypochlorite solution (diluted bleach 1:5) for 3 min, 70% ethanol for 3 min, and briefly in autoclaved water. In groups of two, four pupae were placed in a 47 mm dish containing 4 ml of Grace's insect medium (Gibco, Thermo Fisher Scientific) supplemented with 10% heat-treated fetal bovine serum (FBS, Corning, NY, USA) and 2.5% antibiotic/antimycotic mix (A5955, Sigma Aldrich). Thorax and abdomen of pupae were opened dorsally using sterile forceps to vigorously disturb tissues and release cells into the medium. The medium containing hemolymph cells was filtered using a cell strainer (Corning Cell Strainer, 40 µm Nylon, Corning) to remove fat bodies and other debris and transferred to a 50 ml conical tube, where cells were pooled. A total of 15 ml of media (containing cells from 15 pupae) was centrifuged at 500 g (swing arms) at RT for 15 min to collect cells. Cells were then suspended in 1 ml of culture medium and centrifuged at 300 g for 5 min (swing arms). This washing step was repeated once more, and the cells were suspended in 1 ml of culture medium. Resuspended cells (100 µl) were dispensed into a well of a 96-well tissue culture plate (Costar 3595, Corning), which was sealed with parafilm tape and incubated at 32 ± 1 °C, 60 ± 2% relative humidity, under dark conditions.

argK silencing and DWV infection in vitro

To investigate the effect of *argK* silencing on DWV infection, dsRNA (1 µg/well) was applied to day 0 cells (the start of the ex vivo procedure). On day 3, the cells were inoculated with 1×10^5 total-DWV copies, and the cells were harvested on day 5.

Cell viability was assessed using the trypan blue exclusion assay as previously described [94], but with slight modifications. Briefly, 50 µl of 0.4% trypan blue stain solution (Gibco, Thermo Fisher Scientific) were added to cells directly into a well of the plate. After 5 min of incubation, non-adherent cells and medium were aspirated using a micropipette, and adherent cells were washed twice with 200 µl of 1X PBS. Cells adherent to the well bottom were submerged with 100 µl of 1X PBS and observed under an inverted microscope (Axiovert 135, Zeiss).

To isolate RNA from cultured adherent (living) cells, the wells were gently washed twice with 200 µl of 1X PBS to remove viral particles and non-adherent cells. Then, 100 µl of TRIzol reagent (Thermo Fisher Scientific) was added to each well, mixed by pipetting, and the plate was incubated for 10 min at − 80 °C, to promote cell lysis by freeze–thaw. The plates were incubated for 5 min at RT, and the content was transferred in plastic tubes for RNA extraction.

RNA extraction and RT-qPCR

RNA was extracted using TRIzol reagent (Thermo Fisher Scientific), according to the manufacturer's instructions. The quantity and the quality of total RNA were assessed using a Varioskan Flash spectrophotometer (Thermo Fisher Scientific).

DWV genome and *argK* copies were quantified by using the Power SYBR Green RNA-to-Ct 1-Step Kit (Applied Biosystems) as described elsewhere [47]. All primers used are shown in Additional file 1: S1 Table. Primers for *argK* were designed using Primer-BLAST (https://www.ncbi.nlm.nih.gov/tools/primer-blast/). Due to the co-occurrence of both DWV-A and DWV-B variants in the sampled bees, we used primers targeting a conserved section for multiple DWV variants (total-DWV) [95]. The absolute quantification of total-DWV and *argK* copies was performed by relating the Ct values of unknown samples to established standard curves. Each standard curve was established by plotting the logarithm of ten-fold dilutions of a starting solution containing 0.1 ng of purified PCR product (PureLink PCR Purification Kit, Thermo Fisher Scientific), against the corresponding Ct value as the average of three repetitions. Three standard curves were constructed by using seven to ten dilution points per target (DWV, *argK* and *β-actin*). The PCR efficiency was calculated based on the slope and coefficient of correlation (R^2) of the standard curve, according to the following formula: $E = 10^{(-1/\text{slope})} - 1$ (Additional file 1: S2 Table). Loads of total-DWV and *argK* were expressed as copies per nanogram of total RNA.

Differential relative expression was measured by one-step RT-qPCR, using the Power SYBR Green RNA-to-Ct 1-Step Kit (Applied Biosystems, Carlsbad, CA, USA), according to the manufacturer's instructions. Each reaction was prepared in 20 µl and contained 10 µl RT-qPCR mix 2X, 100 nM of forward and reverse primers, 0.16 µl of 125X RT enzyme mix, DEPC-treated water, and 50 ng of total RNA. In correlation analysis, the amount of total RNA loaded in RT-qPCR reactions ranged between 90 and 400 ng. All samples were analyzed in duplicate on a Step One Real Time PCR System (Applied Biosystems). An RT-qPCR assay for *β-actin* mRNA was used as an internal reference gene marker to normalize between the samples for RNA loading [96–98]. Relative gene expression data were analyzed using the Pfaffl method [99], through a recently published spreadsheet-based protocol [100].

Statistical analyses

To analyze the correlation between DWV load and *argK* expression we used Spearman's rank correlation. Two-way ANOVA, followed by Holm-Sidak post hoc test, was used to analyze *argK* expression in different honey bee tissues and developmental stages. Student's *t*-test was used to analyze the effect of dsRNA treatment on the expression of *argK* and DWV relative abundance, in honey bee cells. All statistical analyses were performed using GraphPad Prism 7.

Abbreviations

ArgK	Arginine kinase protein
argK	Arginine kinase encoding gene
ADP	Adenosine diphosphate
ANOVA	Analysis of variance
ATP	Adenosine triphosphate
C-Ab	Antibody directed against a bacterial protein
CKB	Creatine kinase B
Ct	Cycle threshold
Ctrl	Immunoprecipitation experiments carried out using C-Ab
DEGs	Differentially expressed genes
DWV	Deformed wing virus
DWV-Ab	Antibody directed against different DWV isolates
FDR	False discovery rate
GFP	Green fluorescent protein
GO	Gene ontology
HRP	Horse radish peroxidase
IgG	Immunoglobulin G
IP	Immunoprecipitation experiments carried out using DWV-Ab
IP-MS	Immunoprecipitation followed by mass spectrometry
K_{ATP}	ATP-sensitive inwardly rectifying potassium
KEGG	Kyoto Encyclopedia of Genes and Genomes
LC–MS/MS	Liquid chromatography followed by tandem mass spectrometry
NEB	Newly emerged bee
NNV	Nervous necrosis virus
NF-kB	Nuclear factor kappa-light-chain-enhancer of activated B

	cells
PBS	Phosphate-buffered saline
PBST	Phosphate-buffered saline containing 0.1% Tween® 20
PC	Principal component
PVDF	Polyvinylidene fluoride
qPCR/RT-qPCR	Quantitative PCR/reverse transcription-quantitative PCR
RdRp	RNA-dependent RNA polymerase
RNAi	RNA interference
RNA-seq	RNA sequencing
RT	Room temperature
SDS	Sodium dodecyl sulfate
SDS-PAGE	Sodium dodecyl sulphate–polyacrylamide gel electrophoresis
TBSV	Tomato bushy stunt virus
VP	Viral protein
WSSV	White spot syndrome virus

Supplementary Information

The online version contains supplementary material available at https://doi.org/10.1186/s12915-025-02117-x.

Additional file 1: Supplementary Figures (S1-S3) and Tables (S1-S3).

Additional file 2: Dataset S1. Abundance values for each protein and for each target (IP) and control (Ctrl) sample replicate (R).

Additional file 3: Dataset S2. List of proteins significantly enriched in target versus control IP sample.

Additional file 4: Dataset S3. Clustering of DWV-Ab immunoprecipitated honey bee proteins resulting from DAVID analysis.

Acknowledgements
We thank Fabio Gaeta and Giuseppina Zampi for administrative and technical support .

Authors' contributions
A.B., A.V., S.G., and F.P. designed research; A.B., G.D.L., R. M., S.C., M.C., G.J., S.D.G, and I.D.L., performed research; A.B., S.C., M.C., S.D.G, A.V., S.G., and F.P. data analyses and interpretation; J.d.M. contributed new reagents/analytic tools and revised the manuscript; S.G., and F.P. funds acquisition; and A.B., A.V., S.G. and F.P. wrote the paper. All authors read and approved the final manuscript.

Funding
This work was supported by (i) the Ministry of University and Research, Projects of National Relevance: grant no. 2020T58TA3 (BiPP) and grant No. 2017954WNT (UNICO) and (ii) the European Union Next-GenerationEU [PIANO NAZIONALE DI RIPRESA E RESILIENZA (PNRR)—MISSIONE 4 COMPONENTE 2, INVESTIMENTO 1.4—D.D. 1032 17/06/2022, CN00000022]. This manuscript reflects only the authors' views and opinions; neither the European Union nor the European Commission can be considered responsible for them.

Data availability
The dataset supporting the conclusions of this article are available in the Zenodo repository, https://doi.org/https://doi.org/10.5281/zenodo.12799897 [101]. All mass spectrometry data were deposited to the ProteomeXchange Consortium [102] via the MASSIVE repository with the dataset identifier PXD049721 [103].

Declarations

Ethics approval and consent to participate
Not applicable.

Consent for publication
Not applicable.

Competing interests
The authors declare no competing interests.

Author details
[1]Department of Agricultural Sciences, University of Naples Federico II, Naples, Italy. [2]BAT Center-Interuniversity Center for Studies On Bioinspired Agro-Environmental Technology, University of Naples Federico II, Naples, Italy. [3]Institute of Biosciences and BioResources, National Council of Research of Italy, Naples, Italy. [4]Core Facilities, Istituto Superiore di Sanità (ISS), Rome, Italy. [5]Ministero della Salute, Rome, Italy. [6]Department of Ecology, Swedish University of Agricultural Sciences, Uppsala, Sweden.

Received: 13 September 2024 Accepted: 3 January 2025
Published online: 13 January 2025

References

1. Highfield AC, El Nagar A, Mackinder LCM, Noël LM-LJ, Hall MJ, Martin SJ, et al. Deformed wing virus implicated in overwintering honeybee colony losses. Appl Environ Microbiol. 2009;75:7212–20.
2. Genersch E, Von Der OHE W, Kaatz H, Schroeder A, Otten C, Büchler R, et al. The German bee monitoring project: a long term study to understand periodically high winter losses of honey bee colonies. Apidologie. 2010;41:332–52.
3. Kielmanowicz MG, Inberg A, Lerner IM, Golani Y, Brown N, Turner CL, et al. Prospective large-scale field study generates predictive model identifying major contributors to colony losses. PLOS Pathog. 2015;11: e1004816.
4. Yañez O, Piot N, Dalmon A, de Miranda JR, Chantawannakul P, Panziera D, et al. Bee viruses: routes of infection in hymenoptera. Front Microbiol. 2020;11:943.
5. de Miranda JR, Genersch E. Deformed wing virus. J Invertebr Pathol. 2010;103:S48-61.
6. Wilfert L, Long G, Leggett HC, Schmid-Hempel P, Butlin R, Martin SJM, et al. Deformed wing virus is a recent global epidemic in honeybees driven by *Varroa* mites. Science. 2016;351:594–7.
7. Martin SJ, Brettell LE. Deformed wing virus in honeybees and other insects. Annu Rev Virol. 2019;6:49–69.
8. Traynor KS, Mondet F, de Miranda JR, Techer M, Kowallik V, Oddie MAY, et al. *Varroa destructor*: a complex parasite, crippling honey bees worldwide. Trends Parasitol. 2020;36:592–606.
9. Nazzi F, Pennacchio F. Disentangling multiple interactions in the hive ecosystem. Trends Parasitol. 2014;30:556–61.
10. Brutscher LM, Daughenbaugh KF, Flenniken ML. Antiviral defense mechanisms in honey bees. Curr Opin Insect Sci. 2015;10:71–82.
11. Doublet V, Oddie MAY, Mondet F, Forsgren E, Dahle B, Furuseth-Hansen E, et al. Shift in virus composition in honeybees (Apis mellifera) following worldwide invasion by the parasitic mite and virus vector Varroa destructor. R Soc Open Sci. 2024;11: 231529.
12. Möckel N, Gisder S, Genersch E. Horizontal transmission of deformed wing virus: pathological consequences in adult bees (Apis mellifera) depend on the transmission route. J Gen Virol. 2011;92(Pt 2):370–7.
13. Locke B, Semberg E, Forsgren E, de Miranda JR. Persistence of subclinical deformed wing virus infections in honeybees following Varroa mite removal and a bee population turnover. PLoS ONE. 2017;12: e0180910.
14. Gisder S, Möckel N, Eisenhardt D, Genersch E. In vivo evolution of viral virulence: switching of deformed wing virus between hosts results in virulence changes and sequence shifts. Environ Microbiol. 2018;20:4612–28.
15. Ryabov EV, Childers AK, Lopez D, Grubbs K, Posada-Florez F, Weaver D, et al. Dynamic evolution in the key honey bee pathogen deformed wing virus: novel insights into virulence and competition using reverse genetics. PLOS Biol. 2019;17: e3000502.
16. Nazzi F, Brown SP, Annoscia D, Del Piccolo F, Di Prisco G, Varricchio P, et al. Synergistic parasite-pathogen interactions mediated by host immunity can drive the collapse of honeybee colonies. PLoS Pathog. 2012;8:e1002735.
17. Škubník K, Nováček J, Füzik T, Přidal A, Paxton RJ, Plevka P. Structure of deformed wing virus, a major honey bee pathogen. Proc Natl Acad Sci. 2017;114:3210–5.
18. Škubník K, Sukeník L, Buchta D, Füzik T, Procházková M, Moravcová J, et al. Capsid opening enables genome release of iflaviruses. Sci Adv. 2021;7: eabd7130.

19. Annoscia D, Brown SP, Di Prisco G, De Paoli E, Del Fabbro S, Frizzera D, et al. Haemolymph removal by Varroa mite destabilizes the dynamical interaction between immune effectors and virus in bees, as predicted by Volterra's model. Proc Biol Sci. 2019;286:20190331.
20. Farooq Q ul A, Shaukat Z, Aiman S, Li CH. Protein-protein interactions: methods, databases, and applications in virus-host study. World J Virol. 2021;10:288–300.
21. Hunter W, Ellis J, Vanengelsdorp D, Hayes J, Westervelt D, Glick E, et al. Large-scale field application of RNAi technology reducing Israeli acute paralysis virus disease in honey bees (Apis mellifera, Hymenoptera: Apidae). PLoS Pathog. 2010;6: e1001160.
22. Desai SD, Eu YJ, Whyard S, Currie RW. Reduction in deformed wing virus infection in larval and adult honey bees (Apis mellifera L.) by double-stranded RNA ingestion. Insect Mol Biol. 2012;21:446–55.
23. Smeele ZE, Baty JW, Lester PJ. Effects of deformed wing virus-targeting dsRNA on viral loads in bees parasitised and non-parasitised by Varroa destructor. Viruses. 2023;15: 2259.
24. Lanzi G, de Miranda JR, Boniotti MB, Cameron CE, Lavazza A, Capucci L, et al. Molecular and biological characterization of deformed wing virus of honeybees (Apis mellifera L.). J Virol. 2006;80:4998–5009.
25. Kalynych S, Přidal A, Pálková L, Levdansky Y, de Miranda JR, Plevka P. Virion structure of iflavirus slow bee paralysis virus at 2.6-angstrom resolution. J Virol. 2016;90:7444–55.
26. Huang S, Fei D, Ma Y, Wang C, Shi D, Liu K, et al. Identification of a novel host protein interacting with the structural protein VP2 of deformed wing virus by yeast two-hybrid screening. Virus Res. 2020;286: 198072.
27. Medina-Puche L, Lozano-Durán R. Immunoprecipitation followed by mass spectrometry: an approach for identifying host–viral protein–protein interactions. In: Fontes EPB, Mäkinen K, editors. Plant-Virus Interactions. New York, NY: Springer US; 2024. p. 289–305.
28. Vasconcellos BM, Guimarães Ribeiro V, Campos N do N, da Silva Romão Mota LG, Moreira MF. A comprehensive review of arginine kinase proteins: what we need to know? Biochem Biophys Rep. 2024;40:101837.
29. Keating JA, Striker R. Phosphorylation events during viral infections provide potential therapeutic targets. Rev Med Virol. 2012;22:166–81.
30. Zheng K, Ren Z, Wang Y. Serine-arginine protein kinases and their targets in viral infection and their inhibition. Cell Mol Life Sci. 2023;80:153.
31. De Miranda JR, Brettell LE, Chejanovsky N, Childers AK, Dalmon A, Deboutte W, et al. Cold case: the disappearance of Egypt bee virus, a fourth distinct master strain of deformed wing virus linked to honeybee mortality in 1970's Egypt. Virol J. 2022;19:12.
32. Warsaba R, Stoynov N, Moon K-M, Flibotte S, Foster L, Jan E. Multiple viral protein genome-linked proteins compensate for viral translation in a positive-sense single-stranded RNA virus infection. J Virol. 2022;96: e0069922.
33. Reuscher CM, Barth S, Gockel F, Netsch A, Seitz K, Rümenapf T, et al. Processing of the 3C/D region of the deformed wing virus (DWV). Viruses. 2023;15: 2344.
34. Ma F, Liu Q, Guan G, Li C, Huang J. Arginine kinase of Litopenaeus vannamei involved in white spot syndrome virus infection. Gene. 2014;539:99–106.
35. O'Neal ST, Swale DR, Anderson TD. ATP-sensitive inwardly rectifying potassium channel regulation of viral infections in honey bees. Sci Rep. 2017;7:8668.
36. Fellows CJ, Simone-Finstrom M, Anderson TD, Swale DR. Potassium ion channels as a molecular target to reduce virus infection and mortality of honey bee colonies. Virol J. 2023;20:134.
37. Eleftherianos I, Won S, Chtarbanova S, Squiban B, Ocorr K, Bodmer R, et al. ATP-sensitive potassium channel (KATP)–dependent regulation of cardiotropic viral infections. Proc Natl Acad Sci. 2011;108:12024–9.
38. Kang L, Shi H, Liu X, Zhang C, Yao Q, Wang Y, et al. Arginine kinase is highly expressed in a resistant strain of silkworm (*Bombyx mori*, Lepidoptera): implication of its role in resistance to *Bombyx mori* nucleopolyhedrovirus. Comp Biochem Physiol B Biochem Mol Biol. 2011;158:230–4.
39. Kelly J, Kavanagh K. Caspofungin primes the immune response of the larvae of Galleria mellonella and induces a non-specific antimicrobial response. J Med Microbiol. 2011;60:189–96.
40. Chen H-Q, Yao Q, Bao F, Chen K-P, Liu X-Y, Li J, et al. Comparative proteome analysis of silkworm in its susceptibility and resistance responses to Bombyx mori densonucleosis virus. Intervirology. 2012;55:21–8.
41. Chen X, Yao P, Chu X, Hao L, Guo X, Xu B. Isolation of arginine kinase from Apis cerana cerana and its possible involvement in response to adverse stress. Cell Stress Chaperones. 2015;20:169–83.
42. Neumann P, Carreck NL. Honey bee colony losses. J Apic Res. 2010;49:1–6.
43. Di Prisco G, Cavaliere V, Annoscia D, Varricchio P, Caprio E, Nazzi F, et al. Neonicotinoid clothianidin adversely affects insect immunity and promotes replication of a viral pathogen in honey bees. Proc Natl Acad Sci. 2013;110:18466–71.
44. Di Prisco G, Annoscia D, Margiotta M, Ferrara R, Varricchio P, Zanni V, et al. A mutualistic symbiosis between a parasitic mite and a pathogenic virus undermines honey bee immunity and health. Proc Natl Acad Sci. 2016;113:3203–8.
45. DeGrandi-Hoffman G, Chen Y. Nutrition, immunity and viral infections in honey bees. Curr Opin Insect Sci. 2015;10:170–6.
46. Doublet V, Labarussias M, de Miranda JR, Moritz RFA, Paxton RJ. Bees under stress: sublethal doses of a neonicotinoid pesticide and pathogens interact to elevate honey bee mortality across the life cycle. Environ Microbiol. 2015;17:969–83.
47. Annoscia D, Di Prisco G, Becchimanzi A, Caprio E, Frizzera D, Linguadoca A, et al. Neonicotinoid Clothianidin reduces honey bee immune response and contributes to Varroa mite proliferation. Nat Commun. 2020;11:5887.
48. Ding B, Qin Y, Chen M. Nucleocapsid proteins: roles beyond viral RNA packaging. Wiley Interdiscip Rev RNA. 2016;7:213–26.
49. Organtini LJ, Shingler KL, Ashley RE, Capaldi EA, Durrani K, Dryden KA, et al. Honey bee deformed wing virus structures reveal that conformational changes accompany genome release. J Virol. 2017;91(e01795–16):e01795–816.
50. Sun L, Li M, Ma Y, Huang S, Ma M, Fei D. Interaction between the VP2 protein of deformed wing virus and host snapin protein and its effect on viral replication. Front Microbiol. 2023;14:14.
51. Chuang C, Prasanth KR, Nagy PD. The glycolytic pyruvate kinase is recruited directly into the viral replicase complex to generate ATP for RNA synthesis. Cell Host Microbe. 2017;22:639-652.e7.
52. Prasanth KR, Chuang C, Nagy PD. Co-opting ATP-generating glycolytic enzyme PGK1 phosphoglycerate kinase facilitates the assembly of viral replicase complexes. PLOS Pathog. 2017;13: e1006689.
53. Lin W, Liu Y, Molho M, Zhang S, Wang L, Xie L, et al. Co-opting the fermentation pathway for tombusvirus replication: Compartmentalization of cellular metabolic pathways for rapid ATP generation. PLoS Pathog. 2019;15: e1008092.
54. Molho M, Chuang C, Nagy PD. Co-opting of nonATP-generating glycolytic enzymes for TBSV replication. Virology. 2021;559:15–29.
55. Wolff G, Melia CE, Snijder EJ, Bárcena M. Double-membrane vesicles as platforms for viral replication. Trends Microbiol. 2020;28:1022–33.
56. Ramière C, Rodriguez J, Enache LS, Lotteau V, André P, Diaz O. Activity of hexokinase is increased by its interaction with hepatitis C virus protein NS5A. J Virol. 2014;88:3246–54.
57. Perrin-Cocon L, Kundlacz C, Jacquemin C, Hanoulle X, Aublin-Gex A, Figl M, et al. Domain 2 of hepatitis C virus protein NS5A activates glucokinase and induces lipogenesis in hepatocytes. Int J Mol Sci. 2022;23:919.
58. Uda K, Fujimoto N, Akiyama Y, Mizuta K, Tanaka K, Ellington WR, et al. Evolution of the arginine kinase gene family. Comp Biochem Physiol Part D Genomics Proteomics. 2006;1:209–18.
59. Newsholme EA, Beis I, Leech AR, Zammit VA. The role of creatine kinase and arginine kinase in muscle. Biochem J. 1978;172:533–7.
60. Wallimann T, Wyss M, Brdiczka D, Nicolay K, Eppenberger HM. Intracellular compartmentation, structure and function of creatine kinase isoenzymes in tissues with high and fluctuating energy demands: the "phosphocreatine circuit" for cellular energy homeostasis. Biochem J. 1992;281 (Pt 1) Pt 1:21–40.
61. Ellington WR. Evolution and physiological roles of phosphagen systems. Annu Rev Physiol. 2001;63:289–325.
62. Shah KS, Evans EC, Pizzorno MC. Localization of deformed wing virus (DWV) in the brains of the honeybee, Apis mellifera Linnaeus. Virol J. 2009;6:182.
63. Ando T, Imamura H, Suzuki R, Aizaki H, Watanabe T, Wakita T, et al. Visualization and measurement of ATP levels in living cells replicating hepatitis C virus genome RNA. PLoS Pathog. 2012;8: e1002561.

64. Klumpp K, Ford MJ, Ruigrok RW. Variation in ATP requirement during influenza virus transcription. J Gen Virol. 1998;79(Pt 5):1033–45.
65. Nomaguchi M, Ackermann M, Yon C, You S, Padmanabhan R. De novo synthesis of negative-strand RNA by Dengue virus RNA-dependent RNA polymerase in vitro: nucleotide, primer, and template parameters. J Virol. 2003;77:8831–42.
66. Vreede FT, Gifford H, Brownlee GG. Role of initiating nucleoside triphosphate concentrations in the regulation of influenza virus replication and transcription. J Virol. 2008;82:6902–10.
67. Frick DN, Lam AMI. Understanding helicases as a means of virus control. Curr Pharm Des. 2006;12:1315–38.
68. Gurer C, Höglund A, Höglund S, Luban J. ATPgammaS disrupts human immunodeficiency virus type 1 virion core integrity. J Virol. 2005;79:5557–67.
69. Li PP, Itoh N, Watanabe M, Shi Y, Liu P, Yang H-J, et al. Association of simian virus 40 vp1 with 70-kilodalton heat shock proteins and viral tumor antigens. J Virol. 2009;83:37–46.
70. Miranda MR, Canepa GE, Bouvier LA, Pereira CA. Trypanosoma cruzi: Oxidative stress induces arginine kinase expression. Exp Parasitol. 2006;114:341–4.
71. Yao C-L, Ji P-F, Kong P, Wang Z-Y, Xiang J-H. Arginine kinase from Litopenaeus vannamei: cloning, expression and catalytic properties. Fish Shellfish Immunol. 2009;26:553–8.
72. Zhang N, Meng X, Jiang H, Ge H, Qian K, Zheng Y, et al. Restoration of energy homeostasis under oxidative stress: Duo synergistic AMPK pathways regulating arginine kinases. PLoS Genet. 2023;19: e1010843.
73. Croker B, Crozat K, Berger M, Xia Y, Sovath S, Schaffer L, et al. ATP-sensitive potassium channels mediate survival during infection in mammals and insects. Nat Genet. 2007;39:1453–60.
74. Crawford RM, Ranki HJ, Botting CH, Budas GR, Jovanovic A. Creatine kinase is physically associated with the cardiac ATP-sensitive K+ channel in vivo. FASEB J Off Publ Fed Am Soc Exp Biol. 2002;16:102–4.
75. Kefaloyianni E, Lyssand JS, Moreno C, Delaroche D, Hong M, Fenyö D, et al. A comparative proteomic analysis of the KATP channel complex in different tissue types. Proteomics. 2013;13:368–78.
76. Zingman LV, Hodgson DM, Bast PH, Kane GC, Perez-Terzic C, Gumina RJ, et al. Kir6.2 is required for adaptation to stress. Proc Natl Acad Sci U S A. 2002;99:13278–83.
77. Zingman LV, Hodgson DM, Alekseev AE, Terzic A. Stress without distress: homeostatic role for K(ATP) channels. Mol Psychiatry. 2003;8:253–4.
78. Jeong Nam Y, Kim A, Sung Lee M, Suep Sohn D, Soo LC. KATP channel block inhibits the Toll-like receptor 2-mediated stimulation of NF-κB by suppressing the activation of Akt, mTOR, JNK and p38-MAPK. Eur J Pharmacol. 2017;815:190–201.
79. Wu Y, Yuan X, Li J, Kadowaki T. DWV Infection in vitro Using Honey Bee Pupal Tissue. Front Microbiol. 2021;12.
80. Wang H-R, Zhu W-J, Wang X. Mechanism of inhibition of arginine kinase by flavonoids consistent with thermodynamics of docking simulation. Int J Biol Macromol. 2011;49:985–91.
81. Xu J-D, Jiang H-S, Wei T-D, Zhang K-Y, Wang X-W, Zhao X-F, et al. Interaction of the small GTPase Cdc42 with arginine kinase restricts white spot syndrome virus in shrimp. J Virol. 2017;91:e01916-e2016.
82. Hara H, Aizaki H, Matsuda M, Shinkai-Ouchi F, Inoue Y, Murakami K, et al. Involvement of creatine kinase B in hepatitis C virus genome replication through interaction with the viral NS4A protein. J Virol. 2009;83:5137–47.
83. Huang P-Y, Hsiao H-C, Wang S-W, Lo S-F, Lu M-W, Chen L-L. Screening for the proteins that can interact with grouper nervous necrosis virus capsid protein. Viruses. 2020;12:985.
84. Harlow E, Lane D. Antibodies: a laboratory manual. New York: CSHL Press; 1988.
85. Sherman BT, Hao M, Qiu J, Jiao X, Baseler MW, Lane HC, et al. DAVID: a web server for functional enrichment analysis and functional annotation of gene lists (2021 update). Nucleic Acids Res. 2022;50:W216–21.
86. de Miranda JR, Bailey L, Ball BV, Blanchard P, Budge GE, Chejanovsky N, et al. Standard methods for virus research in Apis mellifera. J Apic Res. 2013;52:1–56.
87. Chen YP, Pettis JS, Collins A, Feldlaufer MF. Prevalence and transmission of honeybee viruses. Appl Environ Microbiol. 2006;72:606–11.
88. Powell JE, Martinson VG, Urban-Mead K, Moran NA. Routes of acquisition of the gut microbiota of the honey bee Apis mellifera. Appl Environ Microbiol. 2014;80:7378–87.
89. Kwong WK, Mancenido AL, Moran NA. Immune system stimulation by the native gut microbiota of honey bees. R Soc Open Sci. 2017;4: 170003.
90. Dosch C, Manigk A, Streicher T, Tehel A, Paxton RJ, Tragust S. The gut microbiota can provide viral tolerance in the honey bee. Microorganisms. 2021;9:871.
91. Caccia S, Astarita F, Barra E, Di Lelio I, Varricchio P, Pennacchio F. Enhancement of Bacillus thuringiensis toxicity by feeding Spodoptera littoralis larvae with bacteria expressing immune suppressive dsRNA. J Pest Sci. 2020;93:303–14.
92. McMenamin AJ, Parekh F, Lawrence V, Flenniken ML. Investigating virus–host interactions in cultured primary honey bee cells. Insects. 2021;12:653.
93. Watanabe K, Yoshiyama M, Akiduki G, Yokoi K, Hoshida H, Kayukawa T, et al. A simple method for ex vivo honey bee cell culture capable of in vitro gene expression analysis. PLoS ONE. 2021;16: e0257770.
94. Becchimanzi A, Avolio M, Di Lelio I, Marinelli A, Varricchio P, Grimaldi A, et al. Host regulation by the ectophagous parasitoid wasp *Bracon nigricans*. J Insect Physiol. 2017;101:73–81.
95. Bradford EL, Christie CR, Campbell EM, Bowman AS. A real-time PCR method for quantification of the total and major variant strains of the deformed wing virus. PLoS ONE. 2017;12: e0190017.
96. Evans JD, Schwarz RS, Chen YP, Budge G, Cornman RS, De la Rua P, et al. Standard methods for molecular research in Apis mellifera. J Apic Res. 2013;52:1–54.
97. Forsgren E, Locke B, Semberg E, Laugen AT, de Miranda JR. Sample preservation, transport and processing strategies for honeybee RNA extraction: Influence on RNA yield, quality, target quantification and data normalization. J Virol Methods. 2017;246:81–9.
98. Pfaffl MW, Tichopad A, Prgomet C, Neuvians TP. Determination of stable housekeeping genes, differentially regulated target genes and sample integrity: BestKeeper – Excel-based tool using pair-wise correlations. Biotechnol Lett. 2004;26:509–15.
99. Pfaffl MW. A new mathematical model for relative quantification in real-time RT-PCR. Nucleic Acids Res. 2001;29: e45.
100. Ng HF, Ngeow YF. A simple spreadsheet-based method for relative quantification using quantitative real-time PCR. Biochem Mol Biol Educ. 2022;50:99–103.
101. Becchimanzi A, De Leva G, Mattossovich R, Camerini S, Casella M, Di Lelio I, et al. Deformed wing virus interacts with host's arginine kinase to enhance viral replication in honey bees. 2024. Zenodo. https://doi.org/10.5281/zenodo.12799897.
102. Deutsch EW, Bandeira N, Perez-Riverol Y, Sharma V, Carver JJ, Mendoza L, et al. The ProteomeXchange consortium at 10 years: 2023 update. Nucleic Acids Res. 2023;51:D1539–48.
103. Casella M. Deformed wing virus interacts with host's arginine kinase to enhance viral replication in honey bees. MassIVE https://doi.org/10.25345/C57W67H2H (2024).

Publisher's Note